*Proceedings of the 7th International Young Geotechnical Engineers Conference – Scott (Ed.)*


# Effect of micro pore structure on the suffusion of wide-grading loose soils

## Influence de la structure des micro-pores sur la suffusion des sols meubles à granulométrie large

Jiayan Nie & **Yifei Cui**
*State Key Laboratory of Hydroscience and Engineering, Tsinghua University, Beijing, China, yifeicui@mail.tsinghua.edu.cn*

Yanzhou Yin
*Key Laboratory of Mountain Hazards and Earth Surface Process, Institute of Mountain Hazards and Environment, Chinese Academy of Sciences, Chengdu, China*
*University of Chinese Academy of Sciences, Beijing, China*

ABSTRACT: The wide-grading loose soils (WGLS) are widely distributed in nature like earthquake-induced landslide deposits. Fine particles within the WGLS can migrate across the soil skeleton made by coarse particles under the infiltration of rainfall, which is often called suffusion. During the suffusion, fine particles will be eroded from the soil or clog in the pores, which leads to the decrease of the soil volume or increase of the pore water pressure, and further induces the initiation of shallow failure and subsequent debris flows. The suffusion mechanism is closely related to the micro pore structure of the WGLS, which remains unclear and also lacks of adequate attention. In this study, the effect of micro pore structure on the suffusion is studied based on one-dimension seepage tests through 3D solid-fluid sequentially coupled model, which adopts the Darcy's Law to simulate fluid flow through a porous medium and calculates the transportation of fine particles based on the Discrete element method. Two types of WGLS consisting of spherical and irregular coarse particles as soil skeleton are adopted. The migration of fine particles within these two samples, and the subsequent micromechanical behaviors are investigated to provide more insights into the effect of pore structure on suffusion.

RÉSUMÉ: Les sols meubles à granulométrie large (WGLS) sont largement répandus dans la nature, par exemple les dépôts de glissements de terrain provoqués par des tremblements de terre. Les particules fines contenues dans les sols meubles à granulométrie large(WGLS) peuvent migrer à travers le squelette du sol constitué de particules grossières sous l'effet de l'infiltration des précipitations, ce que l'on appelle souvent la suffusion. Pendant la suffusion, les particules fines seront érodées du sol ou s'obstrueront dans les pores.Cela conduit à une diminution du volume du sol ou une augmentation de la pression de l'eau interstitielle, et induit davantage l'initiation d'une défaillance superficielle et les coulées de débris ultérieures. Le mécanisme de suffusion est étroitement lié à la structure des micro-pores des sols meubles à granulométrie large(WGLS), ce qui reste peu clair et ne fait pas l'objet d'une attention suffisante. Dans cette recherche, l'influence de la structure des micro-pores sur la suffusion est étudié sur la base de tests d'infiltration unidimensionnels à l'aide d'un modèle 3D solide-fluide à couplage séquentiel. Ces tests adoptent la loi de Darcy pour simuler l'écoulement des fluides dans un milieu poreux et pour calculer le transport des particules fines en fonction de la méthode des éléments discrets. Deux types de sols meubles à granulométrie large(WGLS) constitués de particules grossières sphériques et irrégulières comme squelette du sol sont adoptés. La migration des particules fines dans ces deux échantillons et les comportements micro-mécaniques qui en découlent sont étudiés dans le but de mieux comprendre l'influence de la structure des pores sur la suffusion.

KEYWORDS: WGLS; suffusion; micro pore structure; solid-fluid sequentially coupled method; fabric anisotropy

## 1 INTRODUCTION

The wide grading soils with size ranging from 0.001 mm to 100 mm are commonly found in the southwestern mountainous areas of China, e.g., the Wenchuan earthquake-induced landslide deposits (Guo et al 2016). Due to the weak consolidation, these soils are relatively loose and contain a larger number of connected pores between coarse particles (Guo & Cui 2020), which provides enough seepage paths for liquid or migration spaces for fine particles when rainfall occurs. As fines migrate though the soils, the pore structures are enlarged and become less stable, that is, the so called suffusion (Burenkova 1993). Consequently, localized collapses or shallow failures firstly initiate and subsequent debris flows happen. It is, therefore, necessary to explore the mechanisms of suffusion from the perspective of micro pore structure to better understand the initiation of landslides or debris flows induced by suffusion.

Three basic conditions namely material susceptibility, hydraulic potential and stress conditions are required for the initiation and progression of suffusion (Garner & Fannin 2010). In other words, the inherent soil properties (e.g., particle size distribution, fines content, particle shape) determine whether soils can be eroded essentially, while hydraulic and stress conditions (e.g., hydraulic gradient or direction, isotropic or anisotropic stress state) collectively affect the possibility and erosion extent of suffusion. There have been extensive laboratory studies with respect to effects of these macro conditions on the suffusion. For example, Wan & Fell (2008) conducted laboratory tests to assess the potential of internal instability of silt-sand-gravel or clay-silt-sand-gravel soils based on their particle size distribution and improved the corresponding procedures. Chang & Zhang (2011) developed a stress-controlled erosion apparatus to study the effect of stress state on the suffusion of gap graded soils, and found that the maximum erosion rate, the variations in soil permeability, and the total deformation of the soil specimen increase with the increase of deviatoric stress. Ouyang & Takahashi (2015) performed seepage tests to examine the effect of initial fines content on the suffusion and found that the soil with the larger initial fines content showed greater amounts of cumulative eroded soil mass and volumetric strain. Chen (2018) further improved this apparatus to investigate the influence of hydraulic gradient conditions on the loss of fine particles and variations of soil permeability. It was shown that the soil under

cyclic hydraulic loading conditions would experience a much larger amount of particles loss and hence a larger decrease of permeability than that under one-directional hydraulic gradient situation given the same imposed value of hydraulic gradient. Thanks to these valuable and significant laboratory efforts, a series of empirical criteria and erosion laws have been proposed to apply to the practical suffusion related engineering problems (Azadbakht et al 2020; Chang & Zhang 2013; Sibille et al 2015), e.g., assessing the internal stability of soils or predicting the eroded extent after suffusion. However, one challenge that phenomenologically based models must face is that they ignore the micro evolving process occurring within the soils and cannot unravel the micro-mechanisms of suffusion.

Recently, the discrete element method (DEM) coupled with fluid flow has been adopted as an alternative approach to simulate the interactions between soil particles and fluids at the microscopic scale during suffusion, in order to explore the underlying micro-mechanisms (Ahmadi et al 2020; Hu et al 2020; Kawano et al 2018; Kanitz & Grabe 2019; Liu et al 2020; Xiong et al 2021; Yin et al 2020; 2021; Zou et al 2020). Among these studies, coarse particle shape of soil skeleton, one of the most important particle properties, has received little attention in the past few decades when simulating suffusion. However, it should be noted that particle shape especially for coarse particles would directly affect the micro pore structure characteristic and further the migration of fine particles. In addition, previous studies have also shown that particle shape has a significant influence on the soil stiffness and shear strength (Shi et al 2020; Nie et al 2020; 2021). Therefore, the main objective of this study is to numerically investigate the effect of micro pore structure resulting from different shape coarse particles (e.g., spherical and realistic shape particles) on the suffusion of wide-grading loose soils. The results would provide evidences for further modification of the current phenomenological erosion model by incorporating into particle shape information.

## 2 NUMERICAL METHOD AND MODELLING

### 2.1 *Solid-fluid sequentially coupled Method*

#### 2.1.1 *DEM and fluid flow equation*

DEM proposed by Cundall and Strack (1979) has been widely adopted to reproduce the complex behaviors of granular soils. In this study, the popular commercial particle flow code (*PFC*$^{3D}$) is employed to solve the motion of particles within gap-graded soil samples during suffusion according to the following equations (Cundall and Strack, 1979):

$$F_i = m\frac{dv_i}{dt} \tag{1a}$$

$$M_i = I_i\frac{d\omega_i}{dt} - (I_j - I_k)\omega_j\omega_k \tag{1b}$$

where *i*, *j*, *k* are subsequent indexes; *m* is the particle mass; $I_i$ is the principal moment of inertia around the *i* direction; $v_i$ and $\omega_i$ are the translation and angular velocities, respectively; $F_i$ and $M_i$ are the resultant force and torque acting on or around the particle centroid, respectively; Eq. (1b) would be simplified as $M_i = I_i\frac{d\omega_i}{dt}$ for spheres in terms of $I_j = I_k$.

A simple linear contact model is adopted here to represent the particle-particle or particle-wall interactions. The corresponding normal and tangential contact forces, denoted as $f_n$ and $f_t$, respectively, are given as the followings (Cundall and Strack, 1979):

$$f_n = \delta k_n \tag{2a}$$

$$f_t = \min\{f_t' + \Delta u k_t, \mu_c f_n\} \tag{2b}$$

where $k_n$ and $k_t$ are the normal and tangential contact stiffness, respectively; $\delta$ and $\Delta u$ are the penetration depth and contact tangential incremental displacement of two contacting particles, respectively; $f_t'$ is the tangential contact force at the previous time step; $\mu_c$ is the contact friction coefficient.

For the computation of fluid flow motion, Darcy's law and mass conservation principles are combined based on the assumption of an incompressible flow within the saturated porous medium to derive the following governing equation (Tang et al 2017):

$$\frac{\partial}{\partial x}\left(k_x\frac{\partial H}{\partial x}\right) + \frac{\partial}{\partial y}\left(k_y\frac{\partial H}{\partial y}\right) + \frac{\partial}{\partial z}\left(k_z\frac{\partial H}{\partial z}\right) + Q = C_w n\gamma_w\frac{\partial H}{\partial t} \tag{3}$$

where *H* is the total fluid head and equals to the sum of pressure and elevation head; $k_x$, $k_y$, $k_z$ are the coefficients of permeability along three principal directions in the Cartesian coordinate system, respectively; $Q$ is the fluid flux; $n$ is the porosity of the porous medium; $C_w$ and $\gamma_w$ are two material parameters, namely the compressibility and unit weight of water, respectively. In this study, they are set as $4.4\times10^{-10}$ Pa$^{-1}$ and 9.8 kN/m$^3$, respectively.

To solve the above fluid flow equation closely, the following head and flow boundary conditions are imposed on the corresponding boundaries (Yin et al 2020):

$$H = H_{bc}(t) \tag{4a}$$

$$\left(k_x\frac{\partial H}{\partial x}\right)n_x + \left(k_y\frac{\partial H}{\partial y}\right)n_y + \left(k_z\frac{\partial H}{\partial z}\right)n_z + q(t) = 0 \tag{4b}$$

where $H_{bc}(t)$ is the total fluid head at the boundary, $q(t)$ is the specified flow rate at the flow boundary; and $n_x$, $n_y$, $n_z$ are the direction cosine of the outward unit normal vector perpendicular to the flow boundary. In this study, the finite difference method is adopted to solve the govern equations, Eqs. (3-4) of fluid flow.

#### 2.1.2 *Effect of fluid on particle movements*

There are mainly three common hydrodynamic forces (e.g., drag, lift and virtual mass forces) acting on the particles during suffusion, and the drag force would be much larger than the lift and virtual mass forces for the relatively small Reynolds number (Kafui et al 2002). Hence, here only the drag force $\boldsymbol{F}_d$ is considered and assumed to act at the center of the particles, and is determined as follows (Tsuji, 1998):

$$\boldsymbol{F}_d = \frac{n}{1-n}\beta V_p\boldsymbol{U}_r \tag{5}$$

where $\boldsymbol{U}_r$ is the relative velocity vector between the particle and the fluid, and $V_p$ is the particle volume; $\beta$ is related to porosity *n*, which can be calculated from (Ergun, 1952):

$$\beta = \begin{cases} 150\mu_w\frac{1-n^2}{d_p^2n^2} + 1.75\frac{(1-n)\rho_0|\boldsymbol{U}_r|}{d_pn^2}, n < 0.8 \\ \frac{3}{4}C_d\frac{|\boldsymbol{U}_r|\rho_0(1-n)n^{-2.7}}{d_p}, n \geq 0.8 \end{cases} \tag{6}$$

where $d_p$ is the fines diameter, $\mu_w$ is the fluid viscosity, $\rho_0$ is the density of the fluid; $C_d$ is related to the particle Reynolds number $Re_p$, which is given as $Re_p = n\rho_0|\boldsymbol{U}_r|d_p/\mu_w$. And,

$$C_d = \begin{cases} \frac{24(1+0.15Re_p^{0.687})}{Re_p}, Re_p < 1000 \\ 0.43, Re_p \geq 1000 \end{cases} \tag{7}$$

2.1.3 *Solid-fluid coupling scheme*

A sequentially coupled scheme is adopted to model the solid-fluid interaction, reference to the previous study (Yin et al 2020, 2021). As shown in Fig. 1, after the model is initialized, the fluid computation mesh porosity ($n$) is calculated to obtain the permeability coefficient ($k$) using the empirical Kozeny-Carman equation (Ergun, 1952):

$$k_x = k_y = k_z = D_{10}^2 n^3 g\rho_0/[150\mu_w(1-n)^2] \quad (8)$$

where $D_{10}$ is the characteristic grain size, and $g$ is the gravitational acceleration.

The acquired permeability coefficients are then imported into the fluid calculation equations, Eqs. (3-4) to obtain the water head distribution. The fluid velocity can be determined using Darcy's law, and then the fluid velocity at any point is calculated by shape functions using an interpolation function. Hence the drag forces are determined based on the fluid velocity and applied to particles. The position and velocity of the fines are then updated.

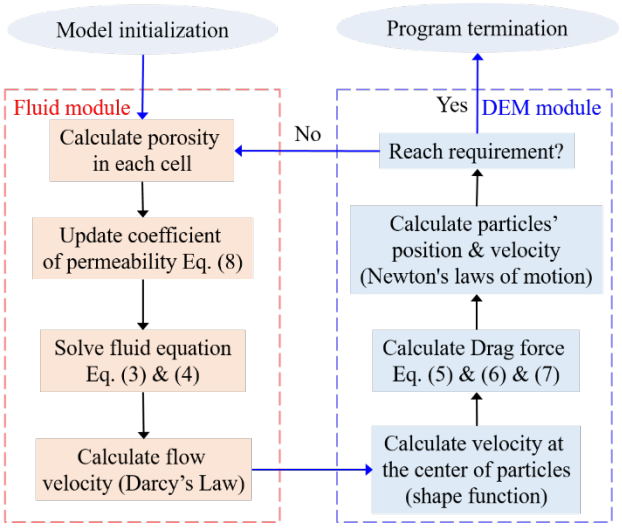


Figure 1. Flowchart of the solid-fluid sequentially coupled met hod

2.2 *One dimensional seepage modelling*

Fig. 2 presents the numerical model configurations of unidirectional seepage tests (downward seepage) conducted in this study. A cubic representative element volume consisting of gap-graded soil particles (binary mixtures including coarse particles with the diameter of 4 mm and fine particles with the diameter of 0.5 mm) is prepared with an initial porosity of 0.36. The fines content in mass is 25%, which means that the initial sample is internally unstable according to Ahmadi et al (2020). In addition, both spherical and realistic shape coarse particles are used so as to explore the effect of shape-induced pore structure on the suffusion. Noted that the particle centroid positions for irregular and spherical coarse particles are kept same in the simulations to ensure comparability. The same shape descriptor named overall regularity (*OR*) with Nie et al (2021) is adopted here to quantify shape differences of both coarse particles (as shown in Fig. 2). Herein the overall regularity is defined as the average of aspect ratio, sphericity and convexity of the coarse particle. For simplicity, the coarse particle is fixed during the whole simulation with the underlying hypothesis that coarse particles skeleton bears most of external load and remains unchanged during suffusion. A subdomain with size of 20 mm (shown in Fig. 2) is chosen as the research area to solve the solid-fluid coupling problem, and the mesh number in this domain is 5×5×5. During simulation, the fine particles whose centroids locate outside this domain are also fixed. At the initial state, a constant inlet flow with velocity of 0.0001 m/s is applied on the top boundary, and the boundary of the bottom is free. And then the migration of fines between coarse particles are analyzed. Table 1 summarizes the adopted model parameters, which have been verified in the previous research (Yin et al 2021). Noted that a local damp mechanism with damping coefficient $\alpha = 0.1$ is adopted in order to reduce violent collisions between particles with high kinetic energy. In this study, the time step for DEM and fluid flow computation are $1.0\times10^{-8}s$ and $1.0\times10^{-7}s$, respectively, which satisfy the computational convergence. The whole computation would be terminated when most of the fluid computation meshes' porosity do not change in 1000 time steps. For the convenience of analysis, the sample with irregular coarse particles is denoted as NS specimen while that with spherical coarse particles is denoted as S specimen in this study.

Table 1. Input parameters used in the solid-fluid sequentially coupled simulation.

| Parameters | *Value* |
|---|---|
| Fine particle diameter $d_f$ (mm) | 0.5 |
| Coarse particle diameter $d_c$ (mm) | 4.0 |
| Particle density $\rho$ (m$^3$/s) | 2650 |
| Contact normal stiffness $k_n$ (N/m) | 1.0× 10$^7$ |
| Contact shear stiffness $k_s$ (N/m) | 1.0× 10$^7$ |
| Contact friction coefficient $\mu_c$ | 1.0 |
| Damping coefficient α | 0.1 |
| Gravitational acceleration $g$ (m/s$^2$) | 9.8 |
| Fluid density $\rho_0$ (m$^3$/s) | 1000 |
| Fluid viscosity $\mu_w$ (Pa·s) | 0.001 |

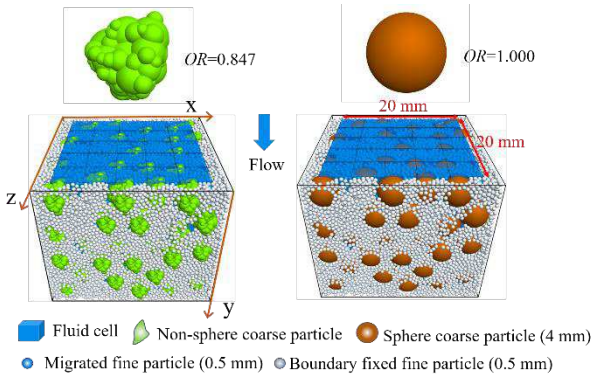


Figure 2. Representative element volume configuration (left: NS specimen, right: S specimen).

## 3 NUMERICAL RESULTS AND DISCUSSIONS

### 3.1 *Loss of fine particles*

Fig. 3(a) gives the evolutions of mass percentages of eroded fines during suffusion for two cases. It can be obviously seen that the amounts of eroded fines firstly increase sharply and then increase with a decreasing rate for both specimens. Moreover, fines within gap-graded soils with spherical coarse particles are eroded out more seriously than those with non-spherical coarse particles. In order to figure out the erosion degrees within different regions of samples along the flow direction, three depth intervals (e.g., the

top region with $y \in [0.00mm, 6.67mm]$, the middle region with $y \in [6.67mm, 13.33mm]$, the bottom region with $y \in [13.33mm, 20.00mm]$) are considered. Fig. 3(b) shows the evolutions of mass percentages of fines within these three regions for two cases, and we can see that for these two samples, fines within the top and bottom regions have almost same evolutions, while there is a big difference in the evolution for the middle part. First, for both samples, comparing the top and bottom regions, the fines within the middle region experience a less decrease of mass percentage due to the supply from the top region. Second, the mass percentage of fines within the middle part of the NS sample changes slightly during suffusion. The possible explanation is that clogging exists extensively within this region when considering the realistic shape of coarse particles, which can be further illustrated in the following section.

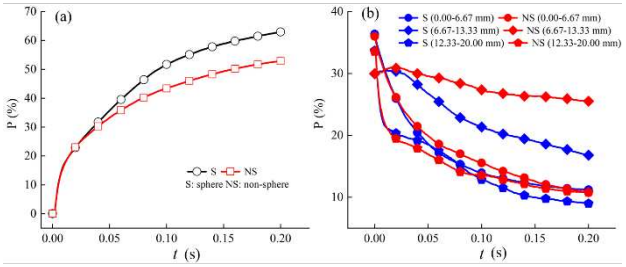


Figure 3. Evolutions of (a): eroded fines mass percentages P for spherical and non-spherical coarse particles cases; (b): mass percentages of fines P within top middle and bottom parts of specimens for these two cases.

### 3.2 *Spatial position and velocity of fines*

To explore the spatial position and velocity of fine particles from the perspective of Euler, Fig. 4 gives the corresponding data for both samples. It can be seen that with the time passing, the fines are eroded more seriously especially within the top and bottom regions of both samples, while the amounts of fines within the middle regions of both samples change not seriously especially for sample with non-spherical coarse particles. An obvious clogging phenomenon has been observed in the middle region of NS specimen (shown in the Figure 4) comparing the fines spatial distributions of NS and S specimens. This is attributed to that the non-spherical coarse particles have reduced the pore size and increased with clogging possibility. In addition, the outlet flow velocity is much larger than that elsewhere during suffusion.

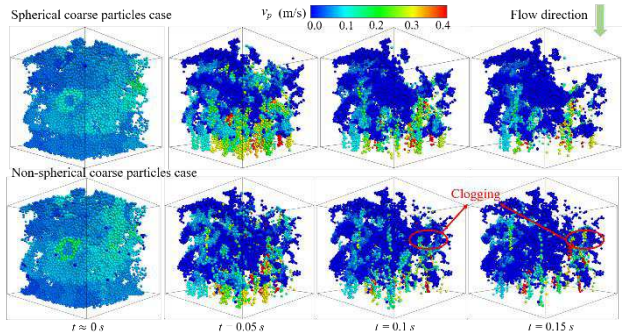


Figure 4. Spatial position and velocity of fines at different times during suffusion for spherical and non-spherical coarse particles cases.

### 3.3 *Contact force chain evolutions*

Consider that fines migration would induce the variation of internal contact network of soils and further change the soil fabric, Fig. 5 shows the contact force chains within both samples and also the corresponding contact normal fabric histograms at different states during suffusion. For both samples, at the initial state, the internal contact force chain networks are anisotropic due to the gravity-induced settlement. However, upon suffusion, the contact normal fabric becomes isotropic, which can be also seen from the uniform contact force chains. This interesting observation suggests that suffusion tends to make the internal soil fabrics more isotropic. The distinct internal contact force chains for both samples highlight the importance of coarse particle shape on the stiffness and shear strength of soils during suffusion. Hence it is necessary to further explore the effect of suffusion on the soil responses from the perspective of "stress-force-fabric" relationship (Ouadfel & Rothenburg 2001) in future research.

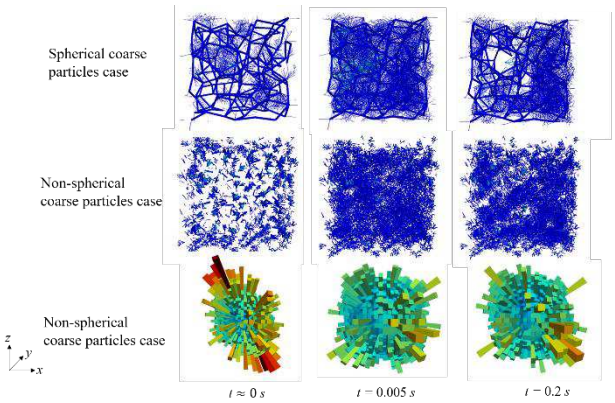


Figure 5. Contact force chain and contact normal anisotropy at different times during suffusion for spherical and non-spherical coarse particles cases.

## 4 CONCLUSIONS

This study attempts to explore the effect of micro pore structure on the suffusion of gap-graded soils based on solid-fluid sequentially coupled numerical simulation. Spherical and non-spherical particles are used to represent the coarse particles, respectively, and hence result in different pore structures. Numerical results show that the amount of eroded fines for sample with non-spherical coarse particles is less than that for sample with spherical coarse particles. Moreover, an obvious clogging phenomenon has been observed in the non-spherical coarse particles sample compared with spherical sample. In addition, suffusion tends to make the soil fabric more isotropic. Hence, it is highly recommended that the "stress-force-fabric" relationship can be adopted as a feasible solution to derive the evolutions of soil strength during suffusion, since fines migration and pore structure evolutions have direct influences on the soil fabric during suffusion.

## 5 ACKNOWLEDGEMENTS

This study was funded by the National Natural Science Foundation of China (42077238) and the Second Tibetan Plateau Scientific Expedition and Research Program (2019QZKK0903). All financial support is gratefully acknowledged.

## 6 REFERENCES

Ahmadi, M., Shire, T., Mehdizadeh, A., & Disfani, M. 2020. DEM modelling to assess internal stability of gap-graded assemblies of spherical particles under various relative densities, fine contents and gap ratios. *Computers and Geotechnics*, 126, 103710.

Azadbakht, S., Nouri, A., & Chan, D. 2020. An analytical model for estimation of internal erosion rate. *Geomechanics and Geoengineering*, 15(1), 42-53.

Burenkova, V. V. 1993. Assessment of suffusion in non-cohesive and graded soils. *Filters in geotechnical and hydraulic engineering. Balkema, Rotterdam*, 357-360.

Chang, D. S., & Zhang, L. M. 2011. A stress-controlled erosion apparatus for studying internal erosion in soils. *Geotechnical Testing Journal*, 34(6), 579-589.

Chang, D. S., & Zhang, L. M. 2013. Extended internal stability criteria for soils under seepage. *Soils and Foundations*, 53(4), 569-583.

Chen, C. 2018. Soil deformation and evolution of stress-strain behaviour induced by internal erosion. *Phd thesis of Hong Kong University of Science and Technology*.

Cundall, P. A., & Strack, O. D. 1979. A discrete numerical model for granular assemblies. *Geotechnique*, 29(1), 47-65.

Ergun, S. 1952. Fluid flow through packed columns. *Journal of Materials Science and Chemical Engineering*, 48(2), 89–94.

Garner, S. J., & Fannin, R. J. 2010. Understanding internal erosion: a decade of research following a sinkhole event. *The international journal on hydropower & dams*, 17(3), 93.

Guo, C., & Cui, Y. 2020. Pore structure characteristics of debris flow source material in the Wenchuan earthquake area. *Engineering Geology*, 267, 105499.

Guo, X., Cui, P., Li, Y., Zhang, J., Ma, L., & Mahoney, W. B. 2016. Spatial features of debris flows and their rainfall thresholds in the Wenchuan earthquake-affected area. *Landslides*, 13(5), 1215-1229.

Hu, Z., Zhang, Y., & Yang, Z. 2020. Suffusion-Induced Evolution of Mechanical and Microstructural Properties of Gap-Graded Soils Using CFD-DEM. *Journal of Geotechnical & Geoenvironmental Engineering*, 146(5), 04020024.

Kanitz, M., & Grabe, J. 2019. Multiscale investigation of suffusion with coupled CFD-DEM: influence of different drag force models. *In Proceedings of the 2nd International Conference on the Material Point Method for Modelling Soil-Water-Structure Interaction*.

Kawano, K., Shire, T., & O'Sullivan, C. 2018. Coupled particle-fluid simulations of the initiation of suffusion. *Soils and foundations*, 58(4), 972-985.

Liu, Y., Wang, L., Hong, Y., Zhao, J., & Yin, Z. Y. 2020. A coupled CFD‐DEM investigation of suffusion of gap graded soil: Coupling effect of confining pressure and fines content. *International Journal for Numerical and Analytical Methods in Geomechanics*, 44(18), 2473-2500.

Nie, J. Y., Cao, Z. J., Li, D. Q., & Cui, Y. F. 2021. 3D DEM insights into the effect of particle overall regularity on macro and micro mechanical behaviours of dense sands. *Computers and Geotechnics*, 132, 103965.

Nie, J. Y., Li, D. Q., Cao, Z. J., Zhou, B., & Zhang, A. J. 2020. Probabilistic characterization and simulation of realistic particle shape based on sphere harmonic representation and Nataf transformation. *Powder Technology*, 360, 209-220.

Ouadfel, H., & Rothenburg, L. 2001. "stress–force–fabric" relationship for assemblies of ellipsoids. *Mechanics of Materials*, 33(4), 201-221.

Ouyang, M., & Takahashi, A. 2015. Influence of initial fines content on fabric of soils subjected to internal erosion. *Canadian Geotechnical Journal*, 53(2), 299-313.

Shi, X. S., Nie, J., Zhao, J., & Gao, Y. 2020. A homogenization equation for the small strain stiffness of gap-graded granular materials. *Computers and Geotechnics*, 121, 103440.

Sibille, L., Marot, D., & Sail, Y. 2015. A description of internal erosion by suffusion and induced settlements on cohesionless granular matter. *Acta Geotechnica*, 10(6), 735-748.

Tang, Y., Chan, D.H., & Zhu, D.Z. 2017. A coupled discrete element model for the simulation of soil and water flow through an orifice. International *Journal for Numerical and Analytical Methods in Geomechanics*, 41(14), 1477-1493.

Tsuji, Y., Kawaguchi, T., & Tanaka, T. 1998. Discrete particle simulation of two-dimensional fluidized bed. *Powder Technology*, 98(1), 79–87.

Wan, C. F., & Fell, R. 2008. Assessing the potential of internal instability and suffusion in embankment dams and their foundations. *Journal of geotechnical & geoenvironmental engineering*, 134(3), 401-407.

Xiong, H., Yin, Z. Y., Zhao, J., & Yang, Y. 2021. Investigating the effect of flow direction on suffusion and its impacts on gap-graded granular soils. *Acta Geotechnica*, 16(2), 399-419.

Yin, Y., Cui, Y., & Jiang, Y. 2020. Microscopic Aspects of Internal Erosion Processes in Gap-Graded Soils. *In The International Conference on Embankment Dams (pp. 267-273). Springer, Cham.*

Yin, Y., Cui, Y., Tang, Y., Liu, D., Lei, M., & Chan, D. 2021. Solid–fluid sequentially coupled simulation of internal erosion of soils due to seepage. *Granular Matter*, 23(2), 1-14.

Zou, Y., Chen, C., & Zhang, L. 2020. Simulating progression of internal erosion in gap-graded sandy gravels using coupled CFD-DEM. *International Journal of Geomechanics*, 20(1), 04019135